JPn Neuroscience

The Journal of Physiology

J Physiol 591.10 (2013) pp 2523–2540

Glutamatergic modulation of synaptic-like vesicle recycling in mechanosensory lanceolate nerve terminals of mammalian hair follicles

Robert W. Banks[1], Peter M. B. Cahusac[2], Anna Graca[3], Nakul Kain[4], Fiona Shenton[1], Paramjeet Singh[3], Arild Njå[5], Anna Simon[3], Sonia Watson[3], Clarke R. Slater[4] and Guy S. Bewick[3]

[1] *School of Biological & Biomedical Sciences, Durham University, Durham DH1 3LE, UK*
[2] *Department of Psychology, University of Stirling, Stirling FK9 4LA, UK*
[3] *School of Medical Sciences, University of Aberdeen, Aberdeen AB25 2ZD, UK*
[4] *Institute of Neuroscience, Newcastle University, Newcastle upon Tyne NE2 4HH, UK*
[5] *Department of Physiology, Institute of Basic Medical Sciences, University of Oslo, N-0317 Oslo, Norway*

Key points

- The lanceolate sensory nerve ending of hair follicles is known to contain small (~50 nm), clear vesicles similar to those of presynaptic terminals, but of unknown function.
- We show that the sensory terminals spontaneously take up and release the fluorescent styryl dye FM1-43, and also provide other evidence that the dye flux is primarily by recycling of these synaptic-like vesicles (SLVs).
- FM1-43 labelling is Ca^{2+} dependent, and its release is sensitive to α-latrotoxin, which is known to deplete synaptic vesicles at neuromuscular junctions.
- Responses of hair follicle afferents are not significantly affected by FM1-43 at a concentration (10 μM) sufficient to label the endings, so the mechanotransduction channel that has previously been shown to be blocked by FM1-43 permeation in hair cells of the inner ear and in cultured dorsal root ganglion cells is either not responsible for sensory transduction in the lanceolate ending or is in some way protected from exposure to the dye.
- The sensory terminals are relatively enriched in glutamate, presumably within the vesicles.
- Exogenous glutamate increases FM1-43 labelling, whereas the labelling is strongly inhibited by PCCG-13, a specific blocker of a non-canonical phospholipase D-linked metabotropic glutamate receptor, but not by canonical ionotropic or metabotropic glutamate receptor blockers. It is also inhibited by FIPI, a novel phospholipase D inhibitor.
- The system of SLVs is closely similar to that we have previously described in the muscle spindle, and where we further demonstrated the regulatory action of glutamate on the sensory response to maintained stretch.
- We conclude that an SLV-mediated glutamatergic system is present in the mechanosensory endings of the primary afferents of lanceolate endings, and it appears to function in a similar way to the autoregulatory system of the muscle spindle.

Abstract Our aim in the present study was to determine whether a glutamatergic modulatory system involving synaptic-like vesicles (SLVs) is present in the lanceolate ending of the mouse and rat hair follicle and, if so, to assess its similarity to that of the rat muscle spindle annulospiral ending we have described previously. Both types of endings are formed by the peripheral sensory terminals of primary mechanosensory dorsal root ganglion cells, so the presence of such a

DOI: 10.1113/jphysiol.2012.243659

system in the lanceolate ending would provide support for our hypothesis that it is a general property of fundamental importance to the regulation of the responsiveness of the broad class of primary mechanosensory endings. We show not only that an SLV-based system is present in lanceolate endings, but also that there are clear parallels between its operation in the two types of mechanosensory endings. In particular, we demonstrate that, as in the muscle spindle: (i) FM1-43 labels the sensory terminals of the lanceolate ending, rather than the closely associated accessory (glial) cells; (ii) the dye enters and leaves the terminals primarily by SLV recycling; (iii) the dye does not block the electrical response to mechanical stimulation, in contrast to its effect on the hair cell and dorsal root ganglion cells in culture; (iv) SLV recycling is Ca^{2+} sensitive; and (v) the sensory terminals are enriched in glutamate. Thus, in the lanceolate sensory ending SLV recycling is itself regulated, at least in part, by glutamate acting through a phospholipase D-coupled metabotropic glutamate receptor.

(Resubmitted 26 August 2012; accepted after revision 21 February 2013; first published online 25 February 2013)
Corresponding author G. S. Bewick: University of Aberdeen, School of Medical Sciences, School of Medical Sciences, Institute of Medical Sciences, Foresterhill, Aberdeen AB25 2ZD, UK. Email: g.s.bewick@abdn.ac.uk

Abbreviations APV, (2R)-amino-5-phosphovaleric acid; 4-CPG, (*S*)-4-carboxyphenylglycine; CPPG, (*RS*)-α-cyclopropyl-4-phosphonophenyl-glycine; DHPG, (*RS*)-3,5-dihydroxyphenylglycine; EAM, external auditory meatus; FIPI, 5-fluoro-2-indolyl des-chlorohalopemide; iGluR, ionotropic glutamate receptor; MCPG, α-methyl-4-carboxyphenylglycine; mGluR, metabotropic glutamate receptor; NFP, neurofilament protein; PCCG-13, 2′-carboxy-3-phenylcyclopropylglycine-13; ROI, region of interest; SK, small-conductance Ca^{2+}-activated K^+ channel; SLV, synaptic-like vesicle; vGluT, vesicular glutamate transporter.

Introduction

The occurrence of small (∼50 nm mean diameter), clear vesicles, indistinguishable ultrastructurally from synaptic vesicles, in the peripheral terminals of vertebrate mechanosensory primary afferents has often been noted, while rarely attracting any further comment (for a review of cutaneous afferents, for example, see Munger & Ide, 1988). Our work on the muscle spindle has led us to refer to them as 'synaptic-like vesicles' (SLVs) in recognition of growing evidence for a close similarity in molecular organization as well as structural appearance between sensory and presynaptic terminal vesicles (Banks *et al.* 2002). The results of labelling primary sensory terminals in spindles with the fluorescent styryl dye FM1-43 (see Betz *et al.* 1992, who also introduced the method in the study of the motor neuromuscular junction) are consistent with the hypothesis that SLVs participate in continuous recycling of terminal membrane (Bewick *et al.* 2005). There, it was shown that static stretch of the spindle enhanced FM1-43 uptake, whereas small-amplitude, high-frequency vibration increased the dye release rate, indicating that this recycling is influenced by activity. Exactly as at chemical synapses, FM1-43 uptake and release in spindle sensory terminals were both sensitive to changes in extracellular calcium and were blocked by divalent metals, such as cobalt, which blocks voltage-gated Ca^{2+} channels.

The similarities between mechansosensory terminal SLVs and vesicles in truly synaptic terminals suggest that there may be a constitutive release of neuroactive substances from this class of sensory nerve terminal, and that this may be enhanced during mechanosensory transduction. This is supported by the observation of relatively high levels of glutamate-like immunoreactivity in the spindle afferent terminals (Bewick *et al.* 2005). In addition, we have shown that exogenous glutamate (>10 μM) increases spindle afferent discharge, and this modulatory effect is abolished by antagonists of a phospholipase D-linked metabotropic glutamate receptor (mGluR), (*R*,*S*)-3,5-dihydroxyphenylglycine (DHPG) and 2′-carboxy-3-phenylcyclopropylglycine-13 (PCCG-13). Furthermore, spindle afferent discharge is substantially reduced, and in some terminals abolished totally, by application of PCCG-13 alone, though not by blockers of the canonical mGluR groups I–III. These findings suggest that endogenous glutamate is released from SLVs of sensory nerve terminals in the spindle and acts on the terminals themselves so as to modulate their excitability.

The main aim of the present study was to investigate whether other mechanosensory endings share the properties of the SLVs in muscle spindles, in particular their proposed role in glutamatergic modulation of the sensory terminal. The lanceolate terminals of sensory axons innervating hair follicles in mammals form palisades around the hair-shaft epithelium and were noticed to contain small, clear vesicles more than 40 years ago (Cauna, 1969). We have used the hairs on the murine pinna to show that membrane cycling occurs in lanceolate endings and is subject to glutamatergic modulation. The similarity of these processes to their counterparts in muscle spindles indicates a fundamentally important role for SLVs

in primary afferent mechanosensory ending function. Preliminary results have been published previously as abstracts (Kain & Slater, 2003; Shenton *et al.* 2009; Singh *et al.* 2009; Graca *et al.* 2010).

Methods

Ethical approval and humane killing

The use of animals in this work has been approved by ethical committees set up according to guidelines from the UK Home Office at the Universities of Aberdeen, Durham, Newcastle and University College London and from the Norwegian Animal Research Authority at the University of Oslo. All animal tissues were obtained after humane killing in accordance with the Animals (Scientific Procedures) Act, 1986. Schedule 1 methods were used, unless specifically stated (see Supplementary Methods).

Light microscopy

Animals and dissection. Adult C57/Bl6J or MF-1 mice (20–45 g; either sex) were used. External ears were removed and pinned in physiological saline (Liley, 1956) saturated with 95% O_2–5% CO_2. Anterior and posterior pinna skin surfaces were separated, cleaned of core cartilage, adipose and connective tissues, then halved to give four equal preparations per mouse before equilibration (1 h, 30°C, bubbled continuously with 95% O_2–5% CO_2).

FM1-43 labelling. Labelling **e**xperiments used a paired (Liley's control *vs.* one or more test solution) standardized incubation protocol (30 min at 30°C, 5 or 10 μM FM1-43 in Liley's/test saline, continuous 95% O_2–5% CO_2 aeration). Dye was washed away (30 min at 30°C, dye-free solution) with Liley's or test solution, as appropriate.

Test solutions. Preparations were first pre-incubated (15–30 min) in dye-free Liley's (control) or appropriate test saline to characterize the following: (i) calcium dependence of FM1-43 labelling; (ii) SLV release; (iii) the role of voltage-dependent calcium channels; (iv) mechanosensory channel inhibitors; and (v) glutamate sensitivity of FM1-43 labelling (see Results and Supplementary Methods for specific solution composition).

Fluorescence microscopy. Epifluorescence images were captured using ×10 or ×40 objectives, with a constant imaging configuration for any particular paired control *vs.* test experiment. See Supplementary Methods for full imaging system details. Images were saved on computer hard drive for later image analysis. The net integrated intensity was determined by subtracting local background from a standard annulus region of interest (ROI; ImageJ; NIH, Bethesda MD, USA) enclosing a complete palisade of endings per follicle (Fig. 1).

Immunocytochemistry. Mouse pinnae were fixed and cryosectioned for immunolabelling against the following antigens: S-100; neurofilament protein; synapsin I; synapsin II; or synaptophysin.

Electrophysiology

We introduced a new *in vitro* preparation for recording the responses of hair follicle afferents to mechanical stimulation of the hair shaft (Fig. 2*A*). Adult mice (C57/Bl6J or Balb/C; 20–35 g) were used. Skin at the base of the skull was removed near the pinnae, exposing the cartilage of the external auditory meatus (EAM) and the innervation of the concave (anterior) and convex (posterior) aspects of pinna skin by branches of the trigeminal (mandibular division) and great auricular nerves, respectively. The EAM was opened anteriorly and the pinna flattened and pinned out,

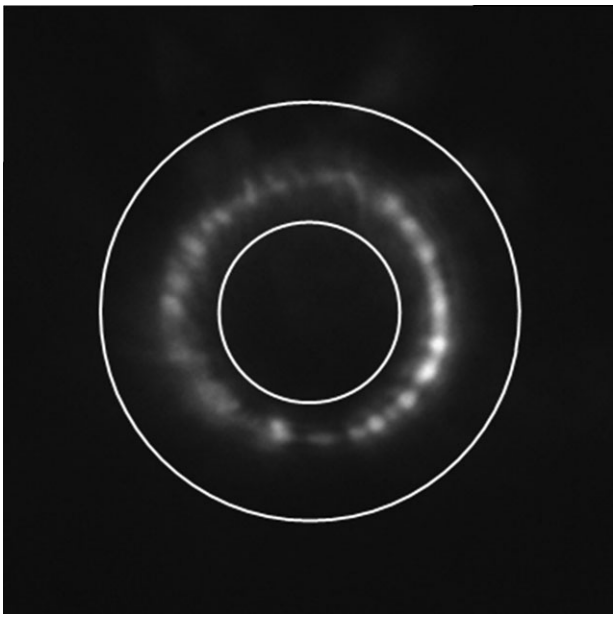

Figure 1. Lanceolate nerve ending in a hair follicle of mouse pinna labelled with FM1-43, showing the annulus used to define a region of interest (ROI) for quantitative analysis of fluorescence intensity
Epifluorescence image. The diameter of the annulus outer circle was set at 30 μm in all experiments. The inner circle diameter was set to ensure that the annulus enclosed all terminals analysed. This was either at 10 μm, as shown here, or at 12.5 μm and kept constant throughout a particular experiment. An annular ROI, rather than a circle, best approximated the area containing terminal labelling and also excluded from the analysis the diffuse autofluorescent spot often found at the base of the hair shaft.

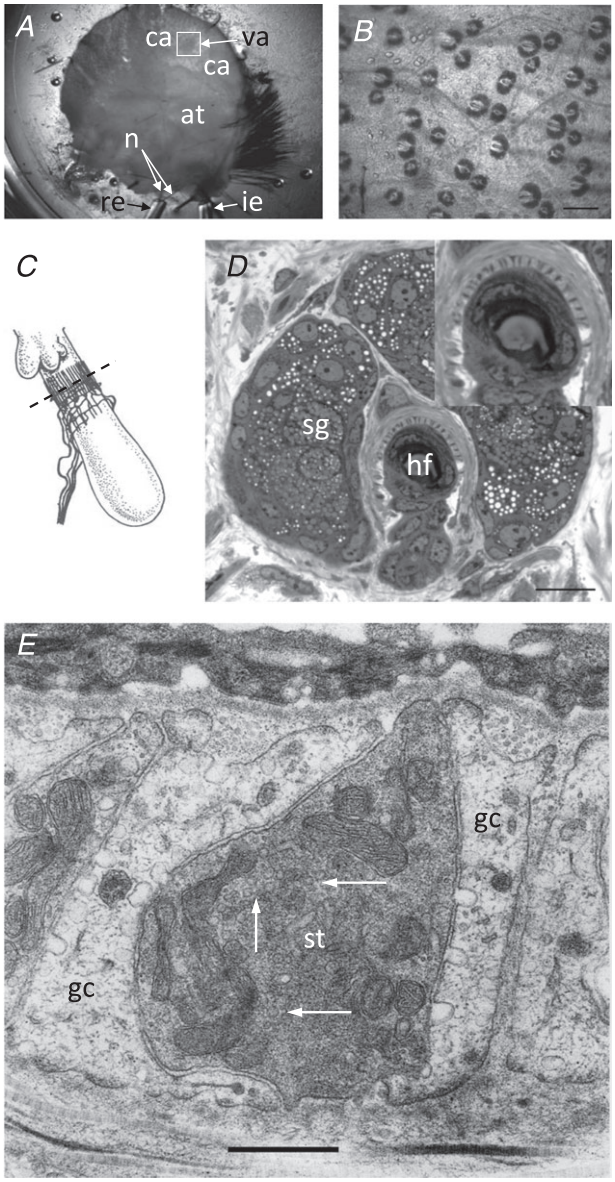

Figure 2. Hair follicles of the anterior skin of the mouse pinna
A, the mouse pinna preparation pinned, anterior skin face down, in a Sylgard-lined dish filled with Liley's solution, and set up for electrophysiological recording. The whole posterior skin has been removed, as well as a large area of elastic cartilage and adipose tissue (at) from the cleared area (ca). By folding the cleared area back, access was gained to the hair shafts, allowing 2 or 3 within the vibrated area (va) to be mechanically displaced by a fire-polished glass capillary (not shown). The nerves (n) are branches of the mandibular division of the trigeminal and are set up for differential recording of the neurogram using recording (re) and indifferent (ie) suction electrodes. *B*, bright-field image of mouse pinna skin viewed from the dermal side, showing several hair follicles. The bases of the hair shafts are clearly seen; each shaft is partly surrounded by a sebaceous gland that appears dark. Scale bar indicates 100 μm. *C*, diagram of the structure and location of the innervation of a hair follicle. The lanceolate ending consists of the group of terminals forming the palisade-like structure immediately below the lobular sebaceous gland (from Bannister, 1976). The dashed line indicates the typical plane of section for subsequent images for fluorescence and light microscopy. *D*, semi-thin (1 μm) cross-section through a hair follicle (hf) at the level of the sebaceous gland (sg) and lanceolate ending, as indicated in *C*. The lanceolate ending surrounds the follicle, and terminals appear as dark structures alternating between lighter accessory cells, shown in greater detail in the inset. Mouse pinna, Toluidine Blue; scale bar (main image) indicates 20 μm. *E*, electron micrograph of an ultrathin cross-section through a lanceolate ending, showing a single, darkly stained, sensory terminal (st) almost completely enclosed by pale-staining glial cell (gc) processes. Note the numerous 50-nm-diameter vesicle profiles in the terminal axoplasm (white arrows). Mouse pinna; scale bar indicates 0.5 μm.

anterior skin down, onto a silicone-lined dish (Sylgard; Dow Corning, Seneffe, Belgium) filled with gassed (95% O_2–5% CO_2) Liley's fluid. Skin of the posterior aspect of the pinna was completely removed and the pinna cartilage partly removed by blunt dissection, leaving the anterior skin intact. Branches (usually two) of the trigeminal mandibular division emerge posteriorly between the pinna and EAM cartilages. They were cleaned and inserted into a glass pipette suction electrode (Fig. 2*A*). A similar pipette was used as the indifferent electrode, whose impedance was balanced using areolar connective tissue. The bath was earthed to the screen of the recording electrode cable. Electrical activity was differentially amplified (Neurolog NL104), filtered (Neurolog NL125; bandpassed 0.2–2 kHz), and recorded using a CED 1401micro interface and Spike2 software (Cambridge Electronic Design, Cambridge, UK) that also controlled a ceramic piezo-electric actuator (PZT507; Morgan Electro Ceramics, Southampton, UK) fitted with a fire-polished 10 cm borosilicate microelectrode glass capillary for mechanical stimulation (3 s at 5 Hz sinusoidal every 30 s) of two or three hairs. Part of the subdermal adipose layer was removed, making a window to the dermis to access follicles for observation or dye application. To stimulate the hairs of these follicles, the edge of the pinna was folded back to expose the external hair shafts, but leaving a small saline-filled gap between the apposed deeper skin layers. The preparations were initially set up in standard Liley's solution, previously gassed with 95% O_2–5% CO_2, which was subsequently changed three times at 10–15 min intervals. This was then followed by 3×10–15 min changes of Liley's solution containing 10 μM FM1-43 and finally one or two changes back to standard Liley's solution. Action-potential-like activity was discriminated using a simple threshold set to approximately 25% of the largest action potentials, which was about twice the high-frequency noise amplitude.

Electron microscopy

Rat and mouse pinna skin and rat cerebellum (positive control) samples were fixed and processed for electron microscopy. For immunogold labelling, ultrathin sections

of rat pinna were labelled postembedding, and particle density was analysed. Rats here provide a direct comparison with our previous work in muscle spindles (Bewick *et al.* 2005).

Statistics

FM1-43 preparations. Each experiment typically involved several different test solutions and a control being prepared simultaneously. Intensity measurement data from the sensory endings of seven to 22 follicles were collected from at least two, and typically three, preparations per experiment (see text/figure legends for individual details, where no. preparations/follicles = d.f. + 1). In some cases, data were normalized to the control mean, taken as 100. Unless otherwise stated, the data were analysed by one-way or two-way ANOVA with replicates, as appropriate, followed by Fisher's least significant difference test. All Students *t* tests were unpaired.

Immunogold preparations. Immunoreactivity was assessed as the number of gold particles per unit area in regions of interest that in general were defined by the profiles of relevant components (sensory terminals, glial cell processes, mossy fibre rosettes, granule cell dendrites and Golgi cell axon terminals) visible in the electron micrographs. The results for the cerebellar cortex, used as positive controls, were closely similar from each animal, so the data from all of the animals were combined and analysed by one-way ANOVA followed by Fisher's least significant difference test.

Results

Preliminary studies showed that isolated samples of mouse ear skin took up FM1-43 in a very distinctive pattern (illustrated here in Fig. 1; first shown by Kain & Slater, 2003). To interpret this pattern, it is first necessary to consider the organization of the palisade structure that forms the basis of the sensory innervation of the hair follicles in this preparation.

Sensory innervation of the hair follicles in mouse pinna skin

When the inner (dermal) surface of the skin was viewed at low magnification, in transmitted light, the bases of numerous hairs were seen (Fig. 2*B*). Each hair was surrounded by a globular sebaceous gland that appeared dark. The innervation of the hair is provided by one or more axons that give rise to numerous (typically 20–30) fine branches running parallel to the axis of the hair shaft, forming a palisade about 10 μm long (Andres, 1966; and Fig. 2*C*). In transverse section, viewed by light microscopy, the palisade appeared as a ring of alternating dark and light segments (Fig. 2*D*). In electron micrographs, the dark segments could be seen to correspond to the individual lanceolate nerve terminals that are rich in mitochondria and also contain many clear vesicles of approximately 50 nm in diameter (Fig. 2*E*). The alternating light profiles corresponded to the arm-like extensions of accessory (Schwann or glial) cells that enwrap the sensory terminals (Andres, 1966).

Identification of the cellular contributions to dark and light segments of the transected palisade was assisted by fluorescence microscopy. Immunolabelling with anti-neurofilament protein (anti-NFP) resulted in a ring of discrete spots, typically about 2–3 μm apart, surrounding the hair shaft (Fig. 3*A*). Similar results were obtained with antibodies against synaptophysin or synapsin I (Fig. 3*B*), two vesicle-associated proteins previously found in sensory nerve terminals in muscle spindles and tendon organs (De Camilli *et al.* 1988), and by direct observation of lanceolate endings in the synaptopHluorin mouse, which reflects the v-SNARE vesicle protein VAMP/synaptobrevin (Fig. 3*C*). After labelling with anti-S-100, a marker of Schwann cells, the pattern was quite different (Fig. 3*D*). In addition to the bright, nucleated cell bodies of the Schwann cells, the ends of the extended arms enwrapping the nerve terminals resulted in horseshoe or paired crescent-shaped regions of immunolabelling, when seen in transverse optical sections through the follicles.

We have recently used synaptophysin-like immunoreactivity as a marker of the spindle sensory terminals in our study on possible components of the mechanotransduction channels (Simon *et al.* 2010). In a double-labelling experiment in the present study, we found that the lanceolate terminals marked by synaptophysin-like immunoreactivity were clearly separate from, while intimately enclosed by, glial cell processes marked by S-100-like immunoreactivity (Fig. 3*E*). We did not find any immunoreactivity against synapsin II, an isoform that is present in many, but not all, synaptic nerve terminals (Kielland *et al.* 2006).

FM1-43 labelling of lanceolate terminals

When isolated skin preparations were immersed in bathing solution containing FM1-43, they acquired a distinctive pattern of labelling. This consisted of numerous rings, typically 20 μm in diameter, of highly fluorescent, elongate spots, each less than 1 μm in minimal diameter (Figs 1, 4*A* and 5*B*). Uptake of the dye occurred without overt experimental stimulation. When a field containing one of the rings was viewed in bright-field illumination, the ring was seen to surround the base

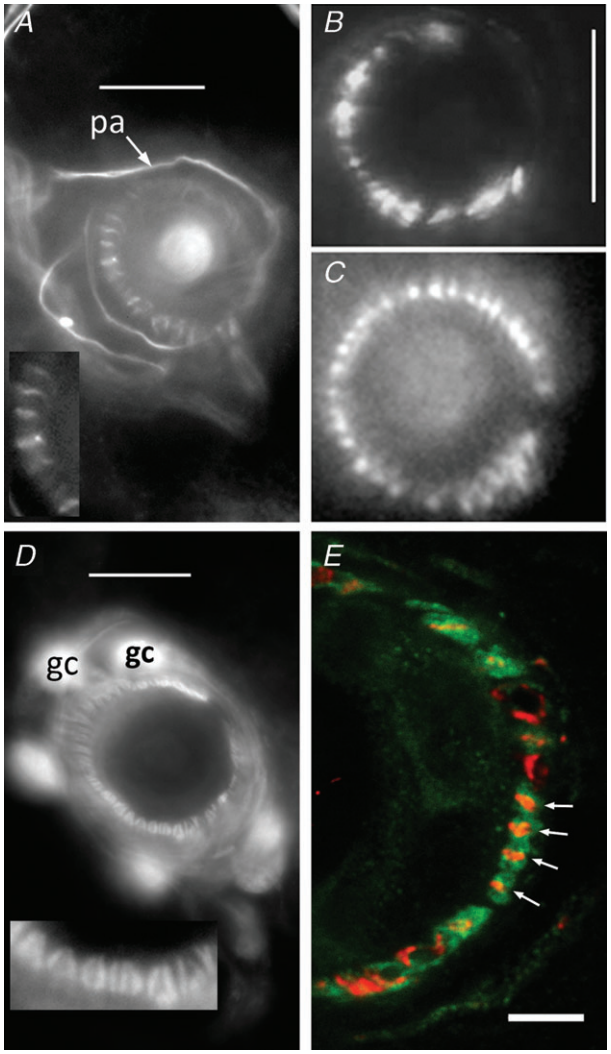

Figure 3. Immunohistochemical and genetic identification of the sensory terminals and glial cells of lanceolate nerve endings
A, anti-neurofilament protein (NFP)-like immunoreactivity is localized in structures identified as preterminal axons (pa) and sensory terminals in a mouse pinna follicle. Several terminals are shown enlarged in the inset. Epifluorescence; scale bar indicates 10 μm. *B*, structures identified as sensory terminals also react strongly with anti-synapsin I antibody. Mouse pinna, epifluorescence; scale bar indicates 20 μm. *C*, synaptopHluorin shows the expression of the v-SNARE synaptobrevin in the lanceolate terminals in a very similar pattern to NFP and synaptophysin. Mouse pinna, epifluorescence; scale as in B. *D*, anti-S-100 antibody, in contrast, labels paired structures identified as glial cells (gc) and their processes in a mouse pinna follicle. Pairing of the processes is particularly apparent in the enlarged inset and is distinct from the unpaired processes seen in *A*. Epifluorescence; scale bar indicates 10 μm. *E*, a follicle from rat pinna double labelled with antibodies against synaptophysin (red) and S-100 (green). Where the ending is precisely orthogonal within the section (white arrows), individual red profiles can be seen clearly to be almost entirely enclosed by paired green profiles, identified as sensory terminals and glial cell processes, respectively. Laser-scanning confocal microscopy; scale bar indicates 5 μm.

of a hair shaft (Fig. S2*A* and *B*). The appearance and distribution of the fluorescent spots were similar to those seen with NFP and synapsin immunolabelling, as well as vesicles labelled directly with green fluorescent protein-tagged VAMP/synaptobrevin (synaptopHluorin, cf. Fig. 1 and Fig. 3*A*–*C*), indicating that they represented FM1-43-labelled lanceolate terminals.

Calcium sensitivity of FM1-43 labelling

Assuming that FM1-43 labelling of lanceolate terminals is predominantly due to incorporation of the dye into SLVs, it would be expected to be Ca^{2+} dependent, as in muscle spindle sensory terminals (Bewick *et al.* 2005). In particular, blocking Ca^{2+} channels or removing Ca^{2+} from the incubation medium should produce a reduction in FM1-43 labelling due to the inhibition of SLV recycling. The addition to the incubation medium of 5 mM Co^{2+}, a broad-spectrum blocker of voltage-dependent Ca^{2+} channels, resulted in an almost 5-fold reduction in fluorescence intensity ($P < 0.001$; Fig. 4*A*–*D*). Replacement of both 2 mM Ca^{2+} and 1 mM Mg^{2+} in standard Liley's solution with 3 mM Co^{2+} produced an even greater reduction in intensity of more than 10-fold ($P < 0.001$; Fig. 4*D*). However, the reduction in intensity following removal of Ca^{2+} and its direct replacement with Mg^{2+} was more modest, to about 55% of control (0 Ca^{2+}/3 mM Mg^{2+} compared with 2 mM Ca^{2+} data not shown; $P < 0.001$), and even in 0 Ca^{2+} in the presence of 1 mM EGTA the intensity was still about 55% of control (Fig. 4*D*; $P < 0.01$).

Voltage-gated Ca^{2+} channels regulating FM1-43 labelling

In order to investigate the type(s) of Ca^{2+} channels present in the lanceolate terminals, we examined the effects of specific channel-blocking toxins. Only modest reductions in fluorescence intensity were produced by the P/Q-type channel blocker ω-agatoxin IVA (0.5 μM) and the N-type channel blocker ω-conotoxin GVIA (5 μM), to 91 and 83% of control values, respectively (both $P < 0.01$; Fig. 4*E*). In contrast, the L-type channel blocker taicatoxin caused much greater reductions in fluorescence intensity, to about 67% of control values in 10 nM toxin (Student's *t* test, $P < 0.001$; Fig. 4*E*). In addition to blocking L-type Ca^{2+} channels, taicatoxin is a potent blocker of small-conductance Ca^{2+}-activated K^+ channels (SK channels; Doorty *et al.* 1997), so we also examined the effect of 1 mM nifedipine, another L-type channel inhibitor, on FM1-43 labelling intensity. Labelling was again reduced to a similar extent, about 58% of control values (Student's *t* test, $P < 0.001$; Fig. 4*E*).

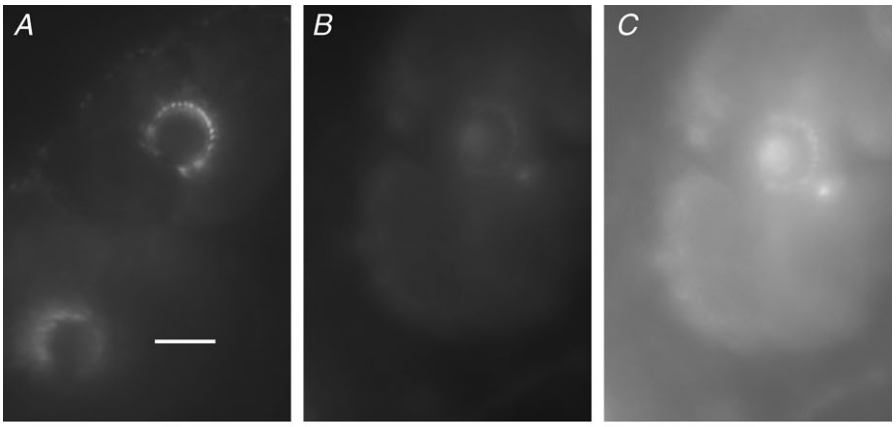

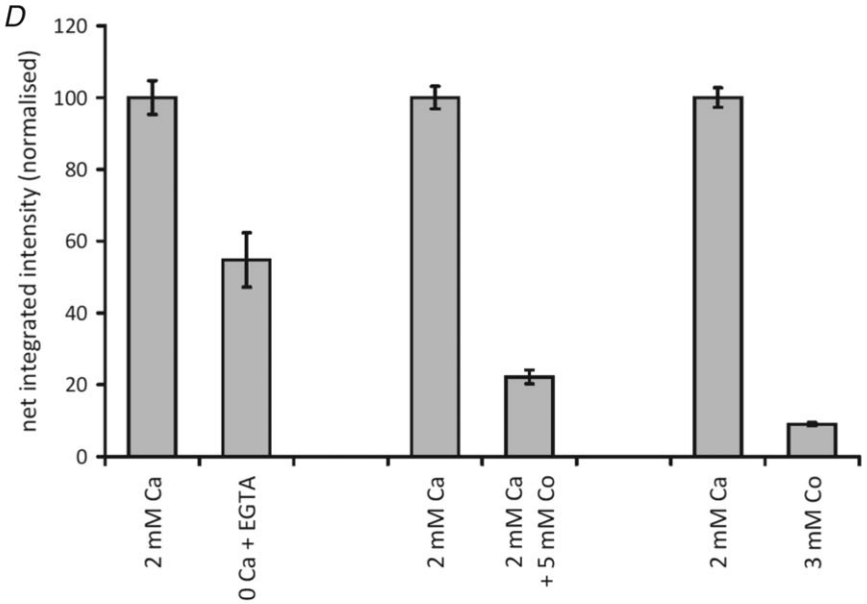

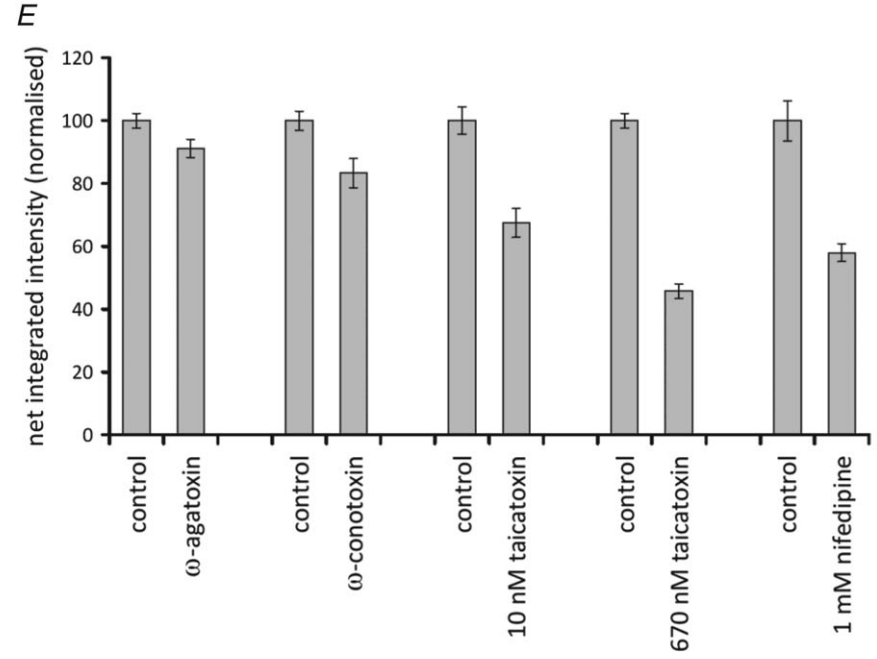

Evidence that sensory terminal labelling occurs predominantly by FM1-43 incorporation into SLVs

The inability of even the most potent of the toxins to reduce FM1-43 labelling by more than 50% highlights the possibility that some of the sensory terminal labelling might be due to a mechanism other than incorporation of the dye into the membranes of SLVs. Specifically, it has been proposed that FM1-43 labelling of vestibulocochlear receptor (hair) cells occurs by permeation of the dye through the open mechanosensitive channels and that, within the cell, the dye is, in essence, irreversibly localized in the membranes of mitochondria and endoplasmic reticulum (Nishikawa & Sasaki, 1996; Gale *et al.* 2001). It was also reported that uptake of the dye in this system is prevented by blockers of the mechanosensitive channels, including high extracellular [Ca^{2+}] (Nishikawa & Sasaki, 1996; Gale *et al.* 2001). However, in the hair follicle lanceolate endings, the spontaneous uptake of FM1-43 was unaffected when the incubation medium included elevated [Ca^{2+}] (5 mM; Fig. 5*A*). The highest external concentration of Ca^{2+} that we used (10 mM) was tested in three experiments, and the results were variable. In one experiment, illustrated here, a small inhibition of FM1-43 labelling was observed (to 88% of control, $P < 0.05$; Fig. 5*A*). In the remaining experiments, however, we found either no significant reduction in labelling or even a small (and significant) increase. Thus, any inhibition by 10 mM Ca^{2+} seemed weak at most.

After transferring FM1-43-labelled preparations to dye-free solution, the terminals of the hair follicle lanceolate endings destained spontaneously (Fig. 5*B*), in contrast to the irreversible staining seen in hair cells. Loss of intensity followed a time course that could be fitted with a single-exponential decay of time constant of approximately 50 min (Fig. 5*C*). When exocytosis was stimulated by 3 nM α-latrotoxin, the rate of loss of the dye was increased more than 2-fold, with a time constant for intensity decay of about 21 min. Intensities were measured at 15 min intervals from 0 to 60 min in both test and control samples, the drug being added to the bathing medium at time 0, and there were significant differences between mean intensities for the test and control samples at each time from 15 to 60 min (Student's *t* test, $P < 0.01$ at 15 min and $P < 0.05$ the rest).

Responses of lanceolate endings to hair shaft movement are highly phasic and are not blocked by FM1-43

Electroneurograms were continuously recorded from three *ex vivo* pinna preparations for periods of between 120 and 150 min each, with mechanical displacement of a few hair shafts (Fig. 6). The amplitude of displacement was ~100 μm, so that peak-to-peak movement of the glass probe was enough to contact some two or three hair shafts during its displacement, but we made no special arrangements to ensure that the probe remained in contact with any particular hair shaft throughout its movement. Nevertheless, responses were remarkably consistent from one 3 s period of vibration to the next, showing only slowly evolving changes over several minutes; at least, until the bathing solution was changed. The preparations were initially set up in standard Liley's solution, previously gassed with 95% O_2–5% CO_2, which was subsequently changed three times at 10–15 min intervals. This was then followed by 3 × 10–15 min changes of Liley's solution containing 10 μM FM1-43 and finally one or two changes back to standard Liley's solution. Action-potential-like activity was discriminated using a simple threshold set to approximately 25% of the largest action potentials, which

Figure 4. FM1-43 labelling of lanceolate endings is Ca^{2+} dependent
A–C, 5 mM Co^{2+} has a strong inhibitory effect on labelling; epifluorescence. *A*, control (2 mM Ca^{2+}); scale bar indicates 20 μm. *B*, 2 mM Ca^{2+} + 5 mM Co^{2+}, imaged in the same conditions as *A*. *C*, the same as *B*, with the brightness of the image greatly increased to show the low level of labelling present. *D*, histograms summarizing the quantitative data on effects of the following permutations: removal of external Ca^{2+} (left two columns); the addition of 5 mM Co^{2+} (middle two columns); and the replacement of external Ca^{2+} with 3 mM Co^{2+} (right two columns). Histograms show means ± SEM. (Statistics for the removal of external Ca^{2+}: 2 pairs of preparations, each of 10 replicates, between preparations, $F_{1,39} = 38.3$, $P < 0.001$; between pairs, $F_1 = 10.3$, $P < 0.01$; statistics for 5 mM Co^{2+}: 4 pairs, 10 replicates, between preparations, $F_{1,79} = 474.2$, $P < 0.001$; between pairs, $F_3 = 1.85$, n.s.; and statistics for replacing Ca^{2+}/Mg^{2+} with 3 mM Co^{2+}: 4 pairs, 10 replicates, between preparations, $F_{1,79} = 1020$, $P < 0.001$; between pairs, $F_3 = 0.15$, n.s.). *E*, in part, the Ca^{2+} dependence of FM1-43 labelling of lanceolate endings is due to L-type channels, as shown by the differential effects of peptide blockers and nifedipine. Histograms (means ± SEM) summarize the quantitative data from separate experiments on the effects (left to right) of the P/Q-type channel blocker ω-agatoxin IVA, the N-type channel blocker ω-conotoxin GVIA, the L-type channel and SK channelblocker taicatoxin, and the L-type channel blocker nifedipine. [Statistics are as follows: (i) ω-agatoxin IVA: 4 pairs, 10 replicates, between preparations, $F_{1,79} = 7.28$, $P < 0.01$; between pairs, $F_3 = 4.48$, $P < 0.01$; (ii) ω-conotoxin GVIA: 4 pairs, 10 replicates, between preparations, $F_{179} = 13.97$, $P < 0.001$; between pairs, $F_3 = 8.3$, $P < 0.001$; (iii) taicatoxin,10 nM, Student's $t = 5.18$, $P < 0.001$ for 71 d.f.; 670 nM, 4 pairs, 10 replicates, between preparations $F_{1,79} = 436.6$, $P < 0.001$; between pairs, $F_3 = 9.33$, $P < 0.001$; and (iv) nifedipine, Student's $t = 6.01$, $P < 0.001$].

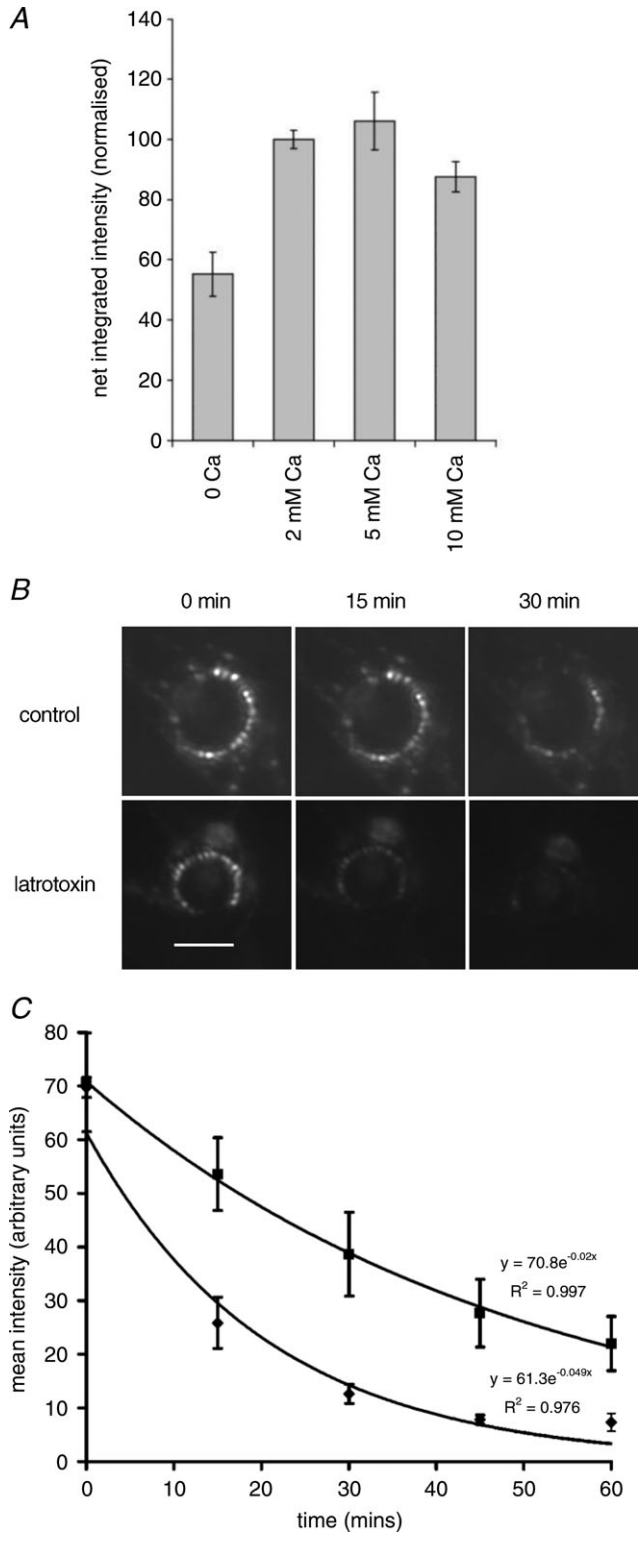

Figure 5. Evidence that little, if any, FM1-43 labelling of lanceolate endings involves permeation of the mechanosensory channel
A, histograms (means ± SEM) summarize the quantitative data from separate experiments on the effects of different levels of external [Ca^{2+}]. There is no, or only weak, inhibition of FM1-43 labelling in the presence of elevated external [Ca^{2+}]. (Statistics for 3 quadruple preparations, 10 replicates, between preparations, $F_{3,119} = 26.1$, $P < 0.001$; between quadruples, $F_2 = 5.11$, $P < 0.01$; Fisher's test *vs.* control, 0 Ca^{2+}/3 mM Mg^{2+}, $P < 0.01$; 5 mM Ca^{2+}, n.s.; and 10 mM Ca^{2+}, $P < 0.05$). *B*, lanceolate endings labelled with FM1-43 destain spontaneously when placed in standard Liley's fluid (control) and more rapidly when placed in Liley's fluid containing 3 nM α-latrotoxin (latrotoxin) to stimulate exocytosis. Epifluorescence; scale bar indicates 20 μm. *C*, the time-dependent loss of fluorescence can be fitted with single-exponent curves. The rate constant in the presence of latrotoxin is more than twice that of the control. Statistical comparison at individual times: Student's *t*, $P < 0.01$ at 15 min and $P < 0.05$ the rest.

was about twice the high-frequency noise amplitude. It is important to note that all the preparations showed ongoing activity even in the absence of imposed movement of the glass-fibre probe, including action potentials of the largest size (Fig. 6*A*). This activity occurred at a rate of about 10–20 impulses s^{-1}, varying more between the preparations ($n = 3$) than from time to time within a preparation; and it showed no structure or signs of tonicity, with the autocorrelation for the intervals between periods of stimulation being quite flat. During mechanical stimulation of the two or three hair shafts, overall output rose to about 20–50 impulses s^{-1}, or four to 10 per sinusoidal cycle (Fig. 6*B*). Construction of cycle histograms revealed strong entrainment, or phase locking, of the response (Fig. 6*E* and *G*). We have not analysed the individual action potentials in detail, but at least in some cases it is clear from discriminable features of spike size and shape that more than one afferent fibre was responding.

The addition of 10 μM FM1-43 had no discernible effect on the spontaneous activity or response of the hair follicle afferents to mechanical displacement, beyond that associated with routine change of bathing solution (Fig. 6*C* and *D*). Thus, although the positions of the peaks in the cycle histograms might change, the responses continued to be highly entrained (Fig. 6*F* and *G*), and a statistical comparison of the last five complete 3 s periods of sinusoidal stimulation in standard Liley's solution prior to the addition of FM1-43, with the last five in the presence of FM1-43 (i.e. after about 45 min exposure to 10 μM dye solution), revealed no significant difference in the numbers of action potentials per cycle (3 preparations with 2 conditions, each of 70 replicates: between preparations, $F_{2,419} = 95.9$, $P < 0.001$; between control and dye treatments, $F_{1,419} = 0.59$, $P = 0.44$, n.s.). At the end of each experiment, hair follicles in the area cleared of adipose tissue, including those stimulated during the electrophysiological recording, were examined for fluorescence, and their lanceolate endings were found to be labelled with FM1-43, showing that dye had indeed penetrated to the terminals (Fig. 6*H* and *I*).

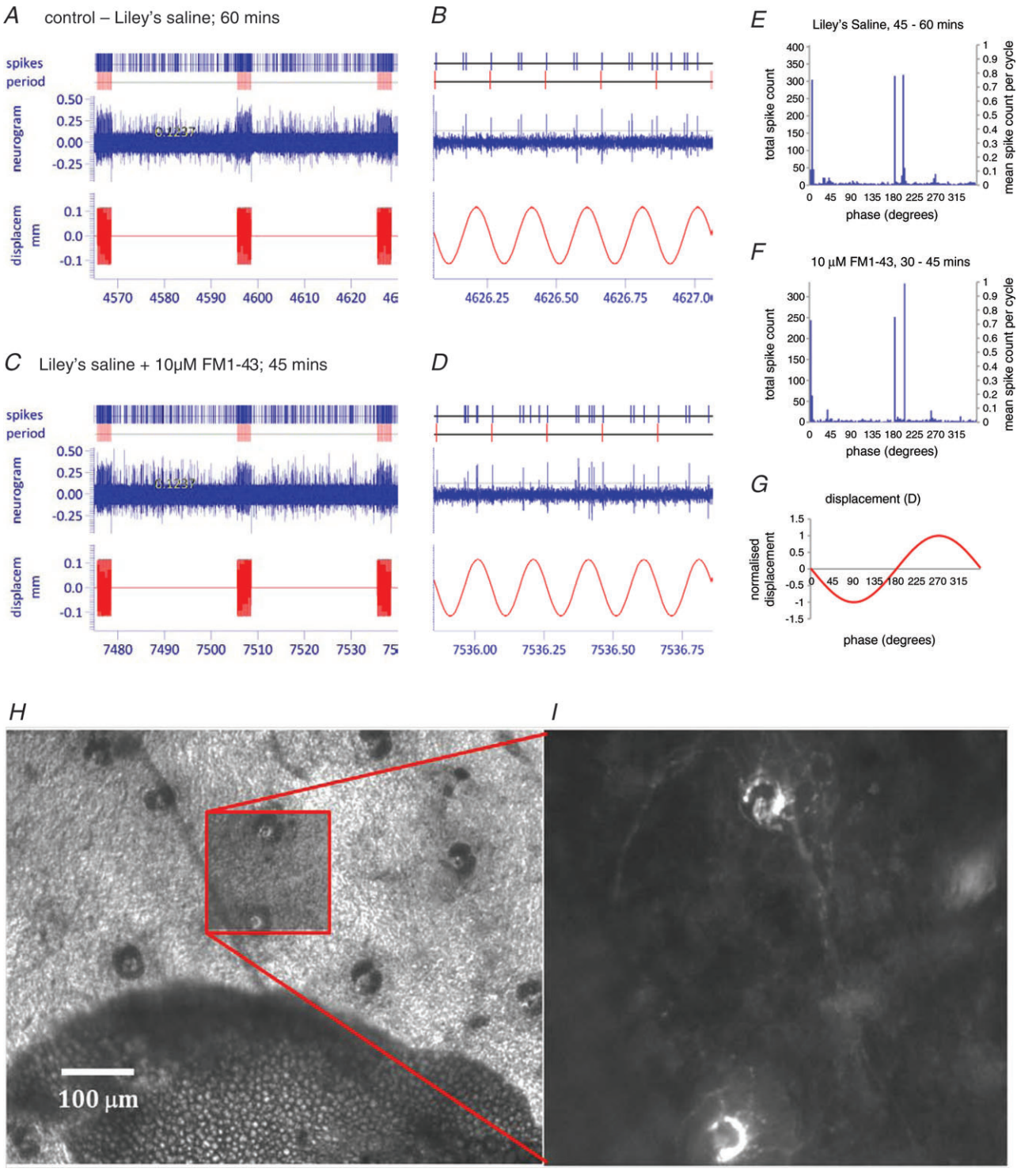

Figure 6. Hair follicle afferent responses are highly phasic and unaffected by 10 μM FM1-43
A and *C*, samples lasting a little over 60 s, including 3 × 3 s periods of sinusoidal displacement of a small number of hair shafts, taken from the continuously recorded neurogram from a single pinna after approximately 60 min in standard Liley's solution (*A*) and after a further 45 min in Liley's solution with 10 μM FM1-43 (*C*). In each case, a 1 s interval from the last period of sinusoidal stimulation is shown on an expanded time scale to the right of the sample (*B* and *D*). Recordings were made with a 1401micro running Spike2 (Cambridge Electronic Design). Custom script files were written to mark individual events that crossed a threshold set by the horizontal cursor, for offline analysis. *E* and *F*, cycle histograms in 3 deg bins constructed from approximately 15 min sections of the neurogram, samples of which are given in *A*–*D*, showing the phase relationships of responses of presumed

Lanceolate endings contain relatively high levels of glutamate

Mechanosensory nerve endings of muscle spindles exhibit levels of glutamate-like immunoreactivity similar to those of known glutamatergic synapses, express vGluT1 vesicular glutamate transporter, and are excited by exogenously applied glutamate (Wu *et al.* 2004; Bewick *et al.* 2005). Excitation by glutamate can be blocked by PCCG-13, a specific blocker of a novel mGluR (Albani-Torregrossa *et al.* 1999), but not by blockers of the canonical glutamate receptors, and there is evidence for constitutive endogenous glutamate release, because application of PCCG-13 alone can completely suppress the response of the endings to stretch (Bewick *et al.* 2005). We therefore investigated whether lanceolate terminals also contain elevated levels of glutamate, and whether a similar glutamatergic action influences FM1-43 staining and destaining of the terminals.

Profiles of lanceolate terminals and their accessory glial cells from hair follicles of pinna skin from four adult rats were sampled for quantification. In addition, mossy fibre terminals, granule cells and Golgi cell axonal terminals of cerebellar cortex were sampled from three of the same animals, the tissue having been processed together with the corresponding skin samples through all stages of fixation, tissue preparation and immunolabelling. The cerebellar material provided positive controls, because it contains readily identifiable, known glutamatergic and GABAergic synapses (Seguela *et al.* 1985; Somogyi *et al.* 1986). Omission of the primary antibodies showed that non-specific reactivity by the 10 nm gold-labelled secondary antibody was negligible. With anti-glutamate primary antibody, labelling (expressed as mean ± SEM gold particles per square micrometre) was much greater in lanceolate terminals (28.2 ± 1.73, $n = 84$) than in the surrounding accessory cells (9.3 ± 0.80, $n = 84$; $P < 0.01$), somewhat higher than in granule cells (22.6 ± 1.13, $n = 45$; $P < 0.01$) and similar to that in mossy fibre terminals (28.2 ± 2.39, $n = 28$) of the cerebellar cortex (Fig. 7*A*–*C*). With anti-GABA primary antibody, no immunoreactivity was found in either the lanceolate terminals or the accessory cells of the skin. However, anti-GABA immunoreactivity was evident in the cerebellum, particularly in Golgi cell axons (Fig. 7*C*).

The action of glutamate on FM1-43 labelling of lanceolate terminals

In the presence of 1 mM glutamate, FM1-43 labelling of the lanceolate terminals in mouse pinna skin was greatly increased (to 178% of control values; Fig. 8). The effect could not be blocked by the addition of a cocktail of ionotropic glutamate receptor (iGluR) and group I–III mGluR blockers (500 μM 4-CPG, 10 μM CPPG and 500 μM kynurenic acid), although the increase in this case (to 143% of control values) was significantly less than that due to glutamate alone. In contrast, the inclusion of only 10 μM PCCG-13 with glutamate not only blocked any glutamate-simulated increase in FM1-43 labelling completely, but also reduced the amount of labelling to 67% of the control mean ($P < 0.001$). Furthermore, in the absence of exogenous glutamate, the addition of PCCG-13 by itself at either 10 or 100 μM reduced labelling substantially when compared with control preparations (to 69 and 53% of control values; $P < 0.05$ and $P < 0.01$, respectively). By contrast, combinations of blockers of iGluRs with group III mGluRs (500 μM kynurenic acid and 10 μM CPPG) or with group I–III mGluRs (500 μM kynurenic acid, 10 μM CPPG and 500 μM 4-CPG) did not significantly change FM1-43 labelling; neither did a group I/II antagonist alone (100 μM MCPG; Fig. 8). The results with LY341495 (a potent inhibitor of canonical mGluRs; Kingston *et al.*, 1998) in the absence of exogenous glutamate depended critically on concentration, as follows. There was a 25% increase in labelling intensity in the presence of 10 μM LY341495 compared with the control mean (4 pairs of preparations, each of 18 replicates: between preparations, $F_{3,143} = 23.1$, $P < 0.001$), but a reduction to 73% of the control mean in the presence of 100 μM LY341495 (5 pairs of preparations, each of 19 replicates: between preparations, $F_{4,189} = 52.2$, $P < 0.001$), a concentration that blocks

lanceolate endings to mechanical stimulation of 2–4 hair shafts by sinusoidal displacement of a glass probe, shown in *G*. Note the marked phase locking in both histograms. *E*, the last change of standard Liley's solution prior to the addition of FM1-43 (406 complete sinusoidal displacements, ending with those in sample *A*). *F*, the last change of Liley's solution containing 10 μM FM1-43 (336 complete sinusoidal displacements, ending with those in sample *D*). *G*, normalized probe displacement; the amplitude was approximately 100 μm (see *A*–*D*). *H* and *I*, part of a pinna preparation at the end of the electrophysiological experiment above showing (*H*) several hair follicles visible in bright-field illumination in the area cleared down to the dermis of the anterior skin. Dark, often bilobed shapes are sebaceous glands. *I*, enlarged view of the area marked by the box in *H* imaged with epifluorescence, showing two lanceolate endings labelled with FM1-43. Hair shafts were accessed by folding the free edge of the pinna over to bring the epidermis of the anterior skin uppermost for mechanical stimulation. Similar results were found in two further preparations.

all cloned mGluRs (Schoepp *et al.* 1999; Wright *et al.* 2000). The involvement of phospholipase D signalling linked to glutamate receptor activation, indicated by the effectiveness of PCCG-13 inhibition, was further supported by the inhibition of FM1-43 labelling in the presence of a novel, potent phospholipase D inhibitor, 5-fluoro-2-indolyl des-chlorohalopemide (FIPI; Su *et al.*, 2009). FM1-43 fluorescence was reduced to 73% of control values in the presence of 100 nM FIPI and to 24% in the presence of 1 μM FIPI (Fig. 8*D* and *E*; $P < 0.01$).

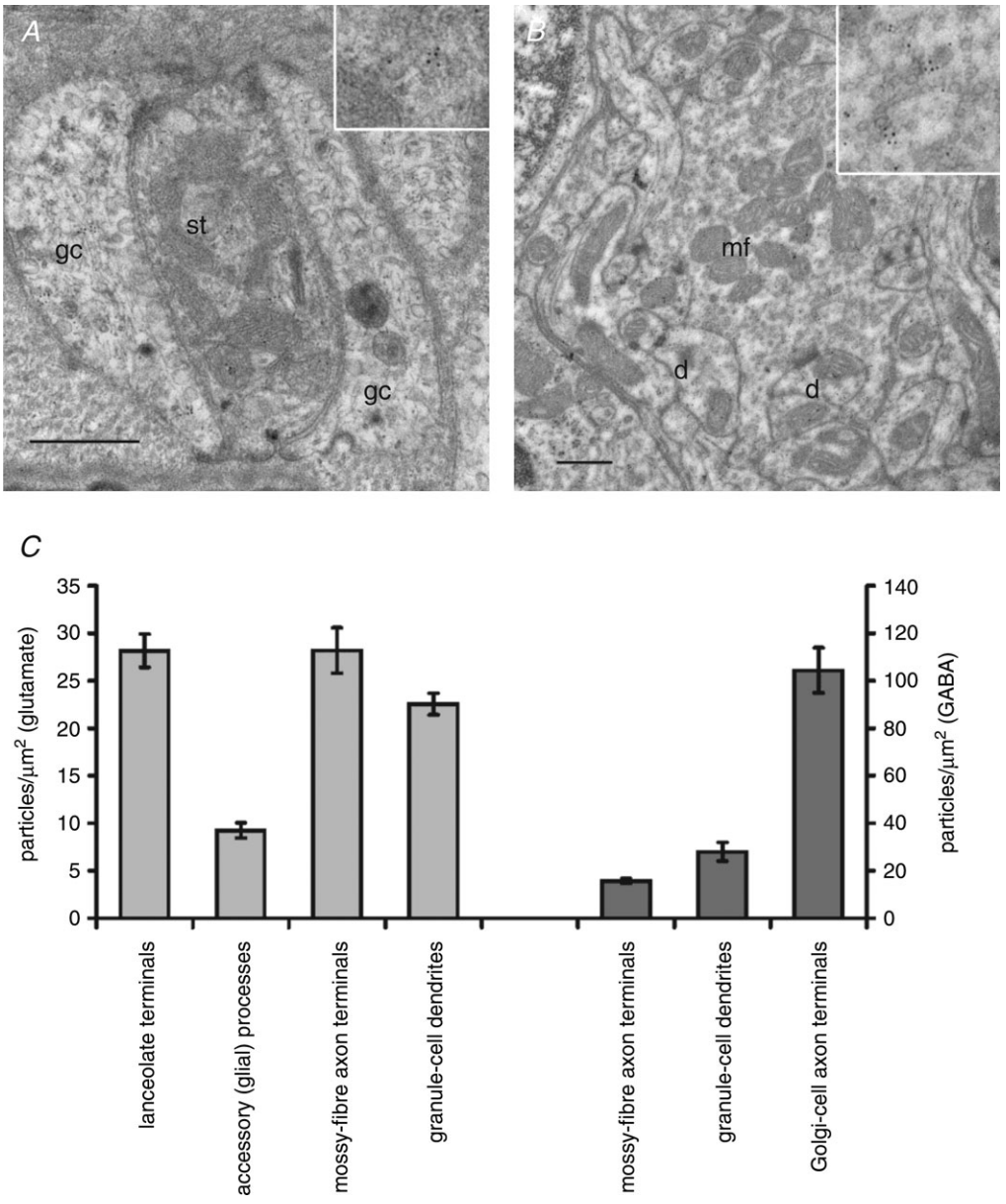

Figure 7. Lanceolate sensory terminals are enriched in glutamate
A and *B*, electron micrographs of thin sections of a sensory lanceolate terminal (st) with enclosing glial cells (gc; *A*) and of a cerebellar cortical synaptic glomerulus (*B*) immunogold labelled to show glutamate-like immunoreactivity. A portion of each is enlarged in the insets, showing gold particles more clearly. The cerebellar glomerulus includes a mossy fibre terminal (mf) and several granule cell dendrites (d). Scale bars (main images) indicate 0.5 μm. *C*, histograms (means ± SEM) summarizing the quantitative assessment of glutamate-like immunoreactivity (light grey; left) and GABA-like immunoreactivity (dark grey; right). No GABA-like immunoreactivity was detected in lanceolate terminals or glial cells. (Statistics for glutamate, $F_{3,240} = 42.6$; Fisher's test *vs.* lanceolate terminals: accessory (glial) cells, $P < 0.01$; mossy fibre terminals, n.s.; and granule cells, $P < 0.01$).

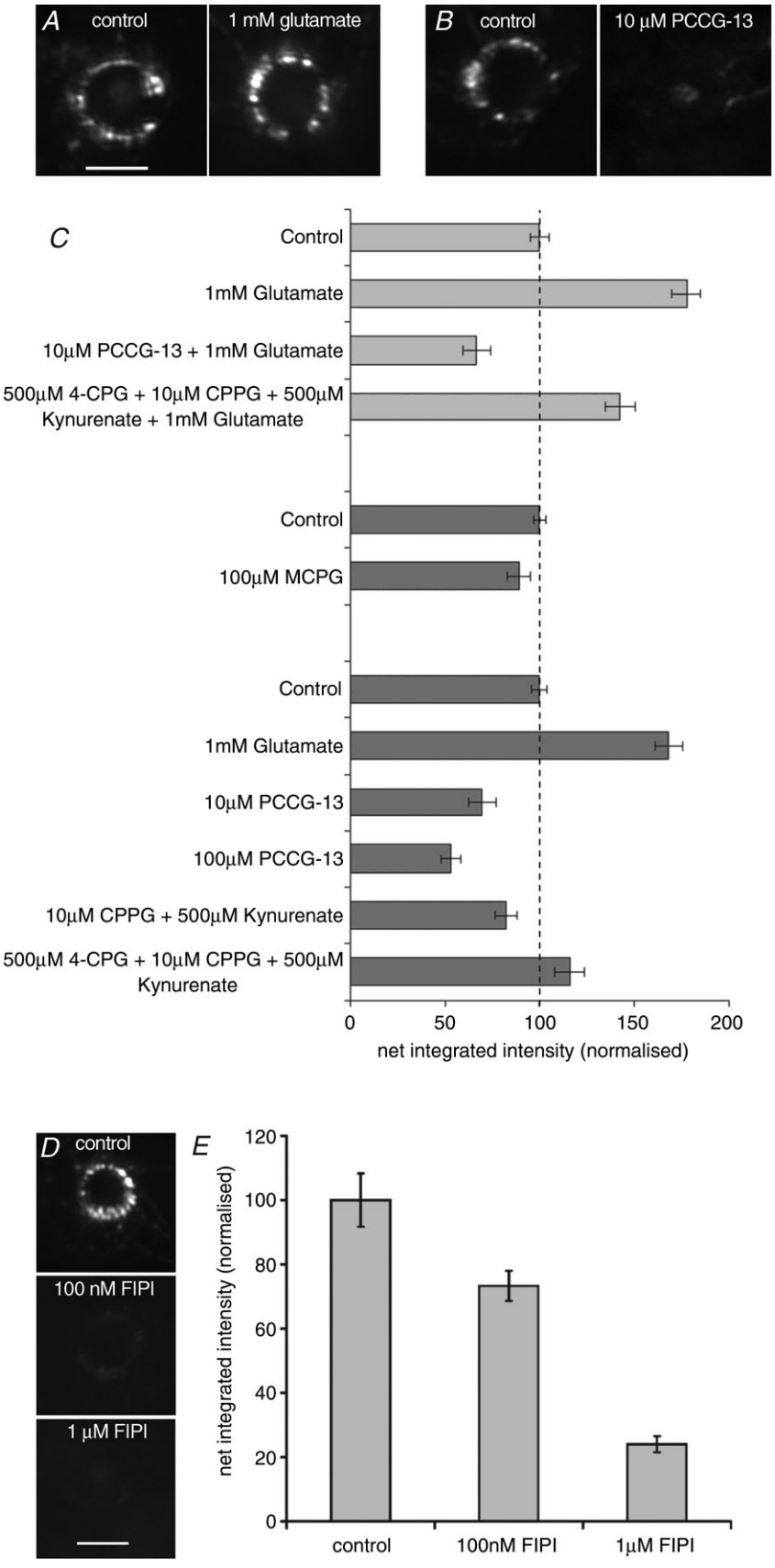

Figure 8. FM1-43 labelling of lanceolate sensory terminals is modulated by glutamate acting through a phospholipase-D-linked metabotropic glutamate receptor (mGluR)
A, FM1-43 labelling is enhanced in the presence of external glutamate. *B*, FM1-43 labelling is reduced in the presence of PCCG-13, a specific blocker of a non-canonical phospholipase-D-linked mGluR. In *A* and *B*, scale bar indicates 20 μm. *C*, histograms (means ± SEM) summarizing the quantitative data on the effects of external glutamate, alone or in the presence of various ionotropic and mGluR blockers (light grey; top) and, in a separate set of experiments, the effects of the blockers alone (dark grey; bottom). PCCG-13 is much more potent than blockers of the canonical glutamate receptors. [Statistics: (i) glutamate and blockers: 2 quadruple preparations, 7 replicates, between preparations, $F_{3,55} = 55.6$, $P < 0.001$; between quadruples, $F_1 = 2.61$, n.s., Fisher's test $P < 0.01$, for all possible comparisons; (ii) MCPG alone: 2 double preparations, 22 replicates, between preparations, $F_{1,87}$, n.s.; (iii) PCCG-13 and blockers of ionotropic glutamate receptor and mGluRs alone: $F_{5,115} = 36.2$, Fisher's test, 10 μM PCCG-13, $P < 0.05$ and 100 μM PCCG-13, $P < 0.01$; all other blockers, n.s.]. *D*, FM1-43 labelling is reduced in the presence of FIPI, an inhibitor of phospholipase D. Scale bar indicates 20 μm. *E*, histograms (means ± SEM) summarizing the quantitative data showing that FIPI caused a dose-dependent decrease in FM1-43 labelling. (Statistics: $F_{2,150} = 24.1$, Fisher's test, all comparisons, $P < 0.01$). *A*, *B* and *D*, epifluorescence.

Discussion

Identification of FM1-43-labelled structures

One of several morphological kinds of low-threshold mechanosensory receptor associated with hair follicles, lanceolate endings occur in all types of follicles from the simplest down (or zigzag; Schlake, 2007) hairs, where they may be the only kind of receptor, to the most complex vibrissae, where they constitute one of a battery of mechanosensory endings (Brown & Iggo, 1967; Luo *et al.* 2009). However, the morphological unity hides an underlying neural diversity, because Aβ, Aδ and C fibres can all terminate as lanceolate endings and, at least in the pelage skin of the trunk, do so in characteristic combinations according to the type of hair follicle, within a single palisade (Li *et al.* 2011). Lanceolate endings supplied by either Aβ or Aδ fibres are rapidly adapting, as were those found by us in the pinna, whereas those supplied by C fibres show intermediate adaptation (Li *et al.* 2011). Like other primary afferent mechanoreceptor endings, including those of the muscle spindle, they contain numerous small vesicles, independently called synaptic-like vesicles (SLVs) by Rice *et al.* (1997) and Banks *et al.* (2002), mainly due to their ultrastructural similarity to the presynaptic vesicles of excitatory synapses. However, the possibility that SLVs might have an important functional role in mechanosensory terminals seems not to have been considered until we demonstrated a glutamatergic neuromodulatory system that arises autogenically from, and acts on, the spindle sensory terminals themselves (Banks *et al.* 2002; Bewick *et al.* 2005). The system is obligatory, because it is possible to abolish reversibly the spindle response to stretch simply by exposure to PCCG-13, a specific blocker of a non-canonical, phospholipase-D-linked mGluR.

Quantitative studies on synaptic vesicle recycling have benefited greatly from the use of fluorescent styryl dyes (Betz & Bewick, 1992; Betz *et al.* 1992), and we have already shown that spindle sensory endings can be labelled with FM1-43 (Banks *et al.* 2002; Bewick *et al.* 2005). Here, we extend our observations on glutamatergic neuromodulation of mechanosensory endings to the lanceolate endings of hair follicles. A major difference between spindle and lanceolate sensory terminals is that the latter are closely invested by pairs of glial cell processes, leaving a narrow cleft where the sensory terminal membrane is exposed to the surrounding connective tissue (Andres, 1966). Although there are numerous SLVs in the sensory terminals, we first had to test the likelihood that FM1-43 was indeed labelling the terminals, rather than the glial processes. Labelled structures were single, more-or-less evenly spaced in a palisade and never continuous with a local cell body; all features expected of the sensory terminals on the basis of ultrastructural studies. Immunoreactivity against NFP, and against the vesicle-associated proteins synaptophysin and synapsin I, resulted in strong fluorescence in axonal profiles and their lanceolate terminals, respectively. In addition, synaptopHluorin fluorescence, reflecting the vesicle-associated v-SNARE VAMP/synaptobrevin, was also strongly expressed in the terminals. All these observations are consistent with the appearance of the FM1-43-labelled structures being terminals and with the idea that both mechanosensory and presynaptic nerve terminals contain similar systems for release and recycling of small vesicles. Conversely, immunoreactivity against S-100, often used as a glial cell marker (Cocchia, 1981), showed more numerous, usually paired, elongate profiles in continuity with local cell bodies, a pattern expected of the glial cell profiles, and quite unlike that of the FM1-43-labelled structures.

FM1-43 labelling is similar in lanceolate and muscle spindle sensory endings, and is at least mainly by vesicle recycling

Our studies on the spindle showed that there was no inhibition of FM1-43 labelling of its sensory endings by high extracellular [Ca^{2+}], unlike the vestibulocochlear receptor (hair) cell, where dye permeation through the mechanosensory channel is so inhibited (Gale *et al.* 2001). Moreover, whereas dye that enters hair cells by channel permeation does not readily exit again (Meyers *et al.* 2003), FM1-43-labelled sensory endings in the spindle destained spontaneously, with increasing rate as the endings were stimulated by high-frequency vibration or latrotoxin (Bewick *et al.* 2005; and G. S. Bewick, unpublished observations). Likewise, in the present study the FM1-43 labelling of the lanceolate endings was inhibited only weakly, if at all, by 10 mM Ca^{2+}, the labelled endings destained spontaneously and, in the presence of 3 nM α-latrotoxin, which specifically increases vesicle exocytosis (Silva *et al.* 2009), the rate of dye loss was increased more than 2-fold. We conclude, therefore, that SLVs in the lanceolate ending undergo a continuous recycling process, exactly as in the spindle. While its failure to inhibit labelling could suggest that elevated Ca^{2+} does not reach the channels, this is unlikely because lowering external Ca^{2+} clearly affects dye uptake (Figs 4*D* and 5*B*). Therefore, given that we do not see any clear evidence for channel permeation of FM1-43 in spindle or lanceolate endings, it would appear that the mechanosensory channels in differentiated neuronal terminals are not the same as in the hair cells. Further evidence in support of this conclusion is provided by our demonstration that FM1-43 at a concentration sufficient to label the lanceolate endings (10 μM) has no discernible effect on the responses of the endings to mechanical displacement, whereas it is a potent blocker of the hair cell mechanosenory currents (Gale *et al.*

2001) and of mechanically sensitive channels in cultured dorsal root ganglion cell bodies (Drew & Wood, 2007) at micromolar concentrations.

Calcium sensitivity of FM1-43 labelling

An essential part of chemical transmission at central and peripheral synapses, the exocytosis of synaptic vesicles, is Ca^{2+} dependent and requires the gating of voltage-dependent Ca^{2+} channels (reviewed by Südhof, 2004). Endocytosis, too, appears to be Ca^{2+} dependent (Lai *et al.* 1999; Wu *et al.* 2009). Consistent with such a mechanism of membrane cycling is the observation that activation of the neuromuscular junction by nerve stimulation or depolarization in the presence of Ca^{2+} is necessary for FM1-43 labelling of terminals to occur (Betz *et al.* 1992). Likewise, destaining of labelled terminals also requires their activation (Betz & Bewick, 1992). In the present study on the sensory (and therefore non-synaptic) terminals of the lanceolate ending, FM1-43 labelling and destaining both occur spontaneously; but, as we have now shown, these too are Ca^{2+} dependent, because labelling is greatly reduced in Ca^{2+}-free solution or in the presence of the non-specific voltage-dependent Ca^{2+} channel blocker Co^{2+}, and the rate of destaining is increased by α-latrotoxin. Once again, these properties of FM1-43 labelling in the lanceolate endings closely resemble those of spindle sensory endings, where exposure to Ca^{2+}-free solutions reduced both labelling and the rates of spontaneous and activity-induced destaining.

The effectiveness of Co^{2+} in inhibiting FM1-43 labelling, whether in the presence or in the absence of external Ca^{2+}, suggests the involvement of voltage-dependent Ca^{2+} channels in the recycling of SLVs in the lanceolate ending. The lesser inhibition of labelling by 0 mM external Ca^{2+} plus EGTA may reflect triggering of Ca^{2+}-induced calcium release from intracellular stores, such as the abundant mitochondria in these terminals (Fig. 2*E*), which can occur in such conditions. The Ca^{2+}-induced calcium release may then support some residual SLV recycling. Conversely, Ca^{2+}-induced calcium release is not believed to be supported by extracellular Co^{2+} (R. H. Scott, personal communication). Labelling was also substantially reduced in the presence of specific blockers of L-type channels, and to a lesser extent by blockers of P/Q- or N-type channels. We do not have directly equivalent data on voltage-dependent Ca^{2+} channels for the spindle, but we have examined the effects of their blockage on firing rates during maintained stretch (Simon *et al.* 2009), which will be reported in full elsewhere. We have also carried out an immunofluorescence study in both spindles and lanceolate endings on SK channels, thought to be associated with these Ca^{2+} channels, which we have prepared for separate publication (Shenton, F., Bewick, G.S. and Banks, R.W. unpublished observations). In our experiments, Ca^{2+} channel blockers were effective even in the absence of vibratory or other mechanical stimulation. It may therefore seem surprising that we have found a role for voltage-dependent channels. While we do not know about the electrical depolarization state of the sensory terminals, we do know that in the *ex vivo* electrophysiological recordings there certainly was spontaneous activity between periods of mechanical stimulation that, on the basis of the sizes of the action potentials, seemed likely to have originated from lanceolate endings. Such activity in the essentially similar *ex vivo* preparation used in the pharmacological experiments could underlie Ca^{2+} channel regulation of SLV recycling.

Evidence for the role of glutamate in the lanceolate endings

We have provided evidence that lanceolate endings exhibit elevated levels of glutamate-like immunoreactivity. In addition, Woo *et al.* (2012) have shown the presence of vGluT2 in lanceolate terminals. This is an interesting contrast with the vGluT1, but not vGluT2, expression in spindle afferent terminals (Wu *et al.* 2004). Nevertheless, both are indicative of a functional role for glutamate loading into vesicles in mechanosensory terminals in general. Consistent with this, as in spindles, immunogold labelling density in the lanceolate sensory terminals was essentially identical to the glutamate-like immunoreactivity of known glutamatergic synapses of the cerebellar cortex, the mossy fibre terminals. In contrast, although GABA-like immunoreactivity was found in Golgi cell axonal terminals of the cerebellar cortex, we found none in the lanceolate endings. A 3-fold lower level of glutamate-like immunoreactivity was found in the accessory cells of lanceolate endings, in comparison to the sensory terminals, but this was still significantly above non-glutamatergic cerebellar components. Like central glia, therefore, the accessory cells may be involved in regulating extracellular glutamate levels and/or recycling it back to the nerve terminal to sustain release. Very recently, indeed, they have been shown to express the NMDA receptor but, perhaps somewhat surprisingly, its prolonged blockage by repeated subcutaneous injections of an (2R)-amino-5-phosphovaleric acid (APV) analogue, CPG 39551, seemed to have little effect on sensory responses of low-threshold afferents to skin indentation even though the accessory cells appeared to be disrupted structurally, at least temporarily (Woo *et al.* 2012).

In the model we have developed, based predominantly on our spindle work (Banks *et al.* 2002; Bewick *et al.* 2005), we suppose that the SLVs contain glutamate, releasing it as they continuously recycle, but at a rate that is, in part at

least, dependent on the mechanoelectrical activity of the sensory ending. The SLV recycling, or glutamate release, or both, are necessary to maintain the responsiveness of the endings to stretch, as evidenced by the following: (i) increase in sensory output to a standard mechanical stimulus in the presence of exogenous glutamate; (ii) prevention of this increase by PCCG-13, a specific blocker of a non-canonical, phospholipase-D-linked mGluR (Albani-Torregrossa *et al.* 1999); and (iii) reversible inhibition of the responsiveness of the sensory endings to mechanical stimulation by PCCG-13 alone, presumably by blocking the maintenance of the sensory response by glutamate released from endogenous sources (i.e. the tonically recycling SLVs). Our recent studies also show a similar glutamate-mediated modulation of firing in aortic baroreceptors through a PCCG-13-sensitive receptor (Paton *et al.* 2010). The present experiments have now allowed us to test whether a similar glutamatergic modulatory system might also occur in lanceolate endings and whether it might affect SLV recycling. We have shown that exogenous application of glutamate (1 mM) during FM1-43 labelling results in a substantial increase in fluorescence compared with control values, which could not be abolished by canonical iGluR or mGluR (group I–III) blockers. However, PCCG-13 entirely prevented the glutamate-induced increase and, indeed, produced a substantial reduction in fluorescence by its application, with or without glutamate, during FM1-43 incubation. In addition, FM1-43 labelling was substantially reduced in the presence of the phospholipase D inhibitor FIPI. As with the spindle, therefore, the action of glutamate appears to be mediated by an atypical phospholipase-D-linked receptor.

It will be immediately clear that our experiments on the effects of glutamate in spindles and lanceolate endings are complementary rather than directly parallel, with each set of experiments providing particular advantages. Thus, the *ex vivo* pinna preparation described here has facilitated observations using FM1-43 fluorescence, whereas the nerve–muscle preparation allowed the detection of relatively small changes in overall firing rates of spindle endings during their tonic responses to stretch. The lanceolate ending is not amenable to the corresponding experiment, owing to its high phasic sensitivity and strong tendency to phase locking to a vibratory stimulus, resulting in serious distortion of the response to a continuous stimulus. In fact, the primary ending of the spindle, which exhibits both dynamic (phasic) and static (tonic) sensitivities, shows similar phase locking that can result in 1:1 'driving' and a complete insensitivity to stretch when stimulated by a small-amplitude vibration or static γ stimulation (Bianconi & van der Meulen, 1963; Banks, 1991).

In conclusion, we have demonstrated the presence in lanceolate endings of a glutamatergic modulatory system of SLVs with properties essentially similar to those of the muscle spindle, where we showed its functional significance in regulating the sensory response of the mechanosensory ending (Bewick *et al.* 2005). The presence of a glutamate-based modulatory system in two different mechanosensory nerve endings is consistent with such autogenic modulation being a ubiquitous feature of primary mechanosensory nerve terminals. This view is further supported by emerging evidence in baroreceptors, and related observations in a crustacean. In the lobster (*Homarus americanus*), the mechanosensory afferent terminals of the oval organ release the neuromodulatory peptide proctolin in a stretch-induced and Ca^{2+}-dependent way (Pasztor *et al.* 1988), and proctolin acts on the same terminals by enhancing their receptor potential and afferent discharge (Pasztor & Bush, 1987, 1989). Finally, we show that in the lanceolate endings, SLV recycling is itself sensitive to glutamatergic control, which is conceivably part of a mechanism for the automatic regulation of mechanosensory excitability.

References

Albani-Torregrossa S, Attucci S, Marinozzi M, Pellicciari R, Moroni F & Pellegrini-Giampietro DE (1999). Antagonist pharmacology of metabotropic glutamate receptors coupled to phospholipase D activation in adult rat hippocampus: focus on (2*R*,1′*S*,2′*R*,3′*S*)-2-(2′-carboxy-3′-phenylcycl opropyl) glycine versus 3,5-dihydroxyphenylglycine. *Mol Pharmacol* **55**, 699–707.

Andres KH (1966). Über die Feinstruktur des Rezeptoren an Sinushaaren. *Z Zellforsch Microsc Anat* **75**, 339–365.

Banks RW (1991). The distribution of static γ-axons in the tenuissimus muscle of the cat. *J Physiol* **442**, 489–512.

Banks RW, Bewick GS, Reid B & Richardson C (2002). Evidence for activity-dependent modulation of sensory-terminal excitability in spindles by glutamate release from synaptic-like vesicles. *Adv Exp Med Biol* **508**, 13–18.

Bannister LH (1976). Sensory terminals of peripheral nerves. In *The Peripheral Nerve*, ed. Landon DH, pp. 369–463. Chapman and Hall, London.

Bianconi R & van der Meulen JP (1963). The responses to vibration of the end-organs of mammalian muscle spindles. *J Neurophysiol* **26**, 177–190.

Betz WJ & Bewick GS (1992). Optical analysis of synaptic vesicle recycling at the frog neuromuscular junction. *Science* **255**, 200–203.

Betz WJ, Mao F & Bewick GS (1992). Activity-dependent fluorescent staining and destaining of living vertebrate motor nerve terminals. *J Neurosci* **12**, 363–375.

Bewick GS, Reid B, Richardson C & Banks RW (2005). Autogenic modulation of mechanoreceptor excitability by glutamate release from synaptic-like vesicles: evidence from the rat muscle spindle primary sensory ending. *J Physiol* **562**, 381–394.

Brown AG & Iggo A (1967). A quantitative study of cutaneous receptors and afferent fibres in the cat and rabbit. *J Physiol* **193**, 707–733.

Cauna N (1969). The fine morphology of the sensory receptor organs in the auricle of the rat. *J Comp Neurol* **136**, 81–98.

Cocchia D (1981). Immunocytochemical localization of S-100 protein in the brain of adult rat. An ultrastructural study. *Cell Tissue Res* **214**, 529–540.

De Camilli P, Vitadello M, Canevini MP, Zanoni R, Jahn R & Gorio A (1988). The synaptic vesicle proteins synapsin I and synaptophysin (protein P38) are concentrated both in efferent and afferent nerve endings of the skeletal muscle. *J Neurosci* **8**, 1625–1631.

Doorty KB, Bevan S, Wadsworth JDF & Strong PN (1997). A novel small conductance Ca^{2+}-activated K^+ channel blocker from *Oxyuranus scutellatus* taipan venom. Re-evaluation of taicatoxin as a selective Ca^{2+} channel probe. *J Biol Chem* **272**, 19925–19930.

Drew LJ & Wood JN (2007). FM1-43 is a permeant blocker of mechanosensitive ion channels in sensory neurons and inhibits behavioral responses to mechanical stimuli. *Mol Pain*, **3**, article 1; Doi: 10.1186/1744-8069-3-1.

Gale JE, Marcotti W, Kennedy HJ, Kros CJ & Richardson GP (2001). FM1-43 dye behaves as a permeant blocker of the hair-cell mechanotransducer channel. *J Neurosci* **21**, 7013–7025.

Graca AB, Singh P, Simon A, Banks RW & Bewick GS (2010). Glutamatergic modulation of synaptic-like vesicle recycling in primary mechanosensory nerve terminals. Program No. 177.3, Poster No. OO8 2010. *Neuroscience Meeting Planner*. Society for Neuroscience, San Diego, CA, 2010. Online. http://www.abstractsonline.com/Plan/ViewAbstract.aspx?sKey=4aa22408-bc97-41d1-8243-6e0b8feb7da6&cKey=530c7738-8f66-4b94-88fe-7a9f4eea8a5f&mKey=%7bE5D5C83F-CE2D-4D71-9DD6-FC7231E090FB%7d. doi 11th March 2013.

Kain N & Slater CR (2003). FM1-43 labelling of mechanosensory endings in mouse skin. *British Neurosci Assoc Abstracts* **17**, P101.

Kielland A, Erisir A, Walaas SI & Heggelund P (2006). Synapsin utilization differs among functional classes of synapses on thalamocortical cells. *J Neurosci* **26**, 5786–5793.

Kingston AE, Ornstein PL, Wright RA, Johnson BG, Mayne NG, Burnett JP, Belagaje R, Wu S & Schoepp DD (1998). LY341495 is a nanomolar potent and selective antagonist of group II metabotropic glutamate receptors. *Neuropharmacol* **37**, 1–12.

Lai MM, Hong JJ, Ruggiero AM, Burnett PE, Slepnev VI, De Camilli P & Snyder SH (1999). The calcineurin-dynamin 1 complex as a calcium sensor for synaptic vesicle endocytosis. *J Biol Chem* **274**, 25963–25966.

Li L, Rutlin M, Abraira VE, Cassidy C, Kus L, Gong S, Jankowski MP, Luo W, Heintz N, Koerber HR, Woodbury CJ & Ginty DD (2011). The functional organization of cutaneous low-threshold mechanosensory neurons. *Cell* **147**, 1615–1627.

Liley AW (1956). An investigation of spontaneous activity at the neuromuscular junction of the rat. *J Physiol* **132**, 650–666.

Luo W, Enomoto H, Rice FL, Milbrandt J & Ginty DD (2009). Molecular identification of rapidly adapting mechanoreceptors and their developmental dependence on Ret signalling. *Neuron* **64**, 841–856.

Meyers JR, MacDonald RB, Duggan A, Lenzi D, Standaert DG, Corwin JT & Corey DP (2003). Lighting up the senses: FM1-43 loading of sensory cells through nonselective ion channels. *J Neurosci* **23**, 4054–4065.

Munger BL & Ide C (1988). The structure and function of cutaneous sensory receptors. *Arch Histol Cytol* **51**, 1–34.

Nishikawa S & Sasaki F (1996). Internalization of styryl dye FM1-43 in the hair cells of lateral line organs in *Xenopus* larvae. *J Histochem Cytochem* **44**, 733–741.

Pasztor VM & Bush BMH (1987). Peripheral modulation of mechanosensitivity in primary afferent neurons. *Nature* **326**, 793–795.

Pasztor VM & Bush BMH (1989). Primary afferent responses of a crustacean mechanoreceptor are modulated by proctolin, octopamine, and serotonin. *J Neurobiol* **20**, 234–254.

Pasztor VM, Lange AB & Orchard I (1988). Stretch-induced release of proctolin from the dendrites of a lobster sense organ. *Brain Res* **458**, 199–203.

Paton JF, Banks RW & Bewick GS (2010). Modulation of afferent excitability and reflex responses by phospholipase D-coupled metabotropic glutamate receptors in the peripheral terminals of rat arterial baroreceptors. *Proc Physiol Soc* **19**, C79.

Rice FL, Fundin BT, Arvidsson J, Aldskogius H & Johansson O (1997). Comprehensive immunofluorescence and lectin binding analysis of vibrissal follicle sinus complex innervation in the mystacial pad of the rat. *J Comp Neurol* **385**, 149–184.

Schlake T (2007). Determination of hair structure and shape. *Semin Cell Dev Biol* **18**, 267–273.

Schoepp DD, Jane DE & Monn JA (1999). Pharmacological agents acting at subtypes of metabotropic glutamate receptors. *Neuropharmacol* **38**, 1431–1476.

Seguela P, Gamrani H, Geffard M, Calas A & Le Moal M (1985). Ultrastructural immunocytochemistry of γ-aminobutyrate in the cerebral and cerebellar cortex of the rat. *Neuroscience* **16**, 865–874.

Shenton FC, Wollner H, Bewick GS & Banks RW (2009). Immunogold labelling for glutamate in lanceolate endings of rat hairs. *Proc Physiol Soc* **17**, 1P.

Silva J-P, Suckling J & Ushkaryov Y (2009). Penelope's web: using α-latrotoxin to untangle the mysteries of exocytosis. *J Neurochem* **111**, 275–290.

Simon A, Banks RW & Bewick GS (2009). KCa channels regulate stretch-evoked afferent firing from muscle spindles. *Proc Physiol Soc* **15**, 28P.

Simon A, Shenton F, Hunter I, Banks RW & Bewick GS (2010). Amiloride-sensitive channels are a major contributor to mechanotransduction in mammalian muscle spindles. *J Physiol* **588**, 171–185.

Singh P, Simon A, Banks RW & Bewick GS (2009). Glutamatergic modulation of vesicle turnover in primary mechanosensory endings. *Proc Physiol Soc* **17**, 1P.

Somogyi P, Halasy K, Somogyi J, Storm-Mathisen J & Ottersen OP (1986). Quantification of immunogold labelling reveals enrichment of glutamate in mossy and parallel fibre terminals in cat cerebellum. *Neuroscience* **19**, 1045–1050.

Su W, Yeku O, Olepu S, Genna A, Park JS, Ren HM, Du G, Gelb MH, Morris AJ & Frohman MA (2009). 5-Fluoro-2-indolyl des-chlorohalopemide (FIPI), a phospholipase D pharmacological inhibitor that alters cell spreading and inhibits chemotaxis. *Mol Pharmacol* **75**, 437–446.

Südhof TC (2004). The synaptic vesicle cycle. *Ann Rev Neurosci* **27**, 509–547.

Woo S-H, Baba Y, Franco AM, Lumpkin EA & Owens DM (2012). Excitatory glutamate is essential for development and maintenance of the piloneural mechanoreceptor. *Development* **139**, 740–748.

Wright RA, Arnold MB, Wheeler WJ, Ornstein PL & Schoepp DD (2000). Binding of [^{3}H](2*S*,1′*S*,2′*S*)-2-(9-xanthylmethyl)-2-(2′-carboxycyclopropyl) glycine ([^{3}H]LY341495) to cell membranes expressing recombinant human group III metabotropic glutamate receptor subtypes. *Naunyn-Schmiedebergs Arch Pharmacol* **362**, 546–554.

Wu S-X, Koshimizu Y, Feng Y-P, Okamoto K, Fujiyama F, Hioki H, Li Y-Q, Kaneko T & Mizuno N (2004). Vesicular glutamate transporter immunoreactivity in the central and peripheral endings of muscle-spindle afferents. *Brain Res* **1011**, 247–251.

Wu X-S, McNeil BD, Xu J, Fan J, Xue L, Melicoff E, Adachi R, Bai L & Wu L-G (2009). Ca^{2+} and calmodulin initiate all forms of endocytosis during depolarization at a nerve terminal. *Nature Neurosci* **12**, 1003–1010.

Author contributions

The experiments were designed by G.S.B., R.W.B., A.N. and C.R.S. and were carried out in their laboratories as follows: G.S.B. (with A.G., A.S., P.S. and S.W., FM1-43 labelling; with R.W.B., P.M.B.C. and SW, electrophysiology), R.W.B. (with F.S., immunofluorescence and immunogold labelling), A.N. (immunofluorescence) and C.R.S. (with N.K., FM1-43 labelling and immunofluorescence). Data were collected by all the authors, as above, but especially by G.S.B., A.G., A.S., P.S., S.W. and F.S., and were finally analysed by R.W.B. All authors contributed to the interpretation of the data. The paper was written by R.W.B. with input from all the other authors, who have approved the final version.

Acknowledgements

We are very grateful to Carol Young for undertaking ultrastructural studies and for assisting with immuno-cytochemical labelling of lanceolate endings in mouse ears. We thank Helen Grindley, Eva Aaboen Hanssen and Christine Richardson for invaluable technical assistance; also Helen Wollner, who assisted with the immunogold labelling for glutamate, Professor Sven Ivar Walaas for gifts of antisynapsin antibodies, Dr Federico Minneci, Professor Angus Silver and Professor David Attwell, University College London for access to synaptopHluorin mouse tissue, Professor Yuri Ushkaryov of the University of Kent for gift of α-latrotoxin and Novartis for gift of FIPI. The work was in part funded by a UK Medical Research Council project grant to G.S.B. and R.W.B., a BioSkape studentship to S.W. from the Scottish Universities Life Sciences Alliance and Eli Lilly, and a Physiological Society Vacation Studentship to A.G., for which we are most grateful.

Authors' present addresses

P. M. B. Cahusac: College of Medicine, Alfaisal University, Riyadh, Saudi Arabia.

A. Graca: Institute of Ophthalmology, University College London, London EC1V 9EL, UK.